

# Analysis of Neural Video Compression Networks for 360-Degree Video Coding

Andy Regensky, Fabian Brand, and André Kaup  
Multimedia Communications and Signal Processing  
Friedrich-Alexander-Universität Erlangen-Nürnberg  
Cauerstr. 7, 91058 Erlangen, Germany  
{andy.regensky, fabian.brand, andre.kaup}@fau.de

**Abstract**—With the increasing efforts of bringing high-quality virtual reality technologies into the market, efficient 360-degree video compression gains in importance. As such, the state-of-the-art H.266/VVC video coding standard integrates dedicated tools for 360-degree video, and considerable efforts have been put into designing 360-degree projection formats with improved compression efficiency. For the fast-evolving field of neural video compression networks (NVCs), the effects of different 360-degree projection formats on the overall compression performance have not yet been investigated. It is thus unclear, whether a resampling from the conventional equirectangular projection (ERP) to other projection formats yields similar gains for NVCs as for hybrid video codecs, and which formats perform best. In this paper, we analyze several generations of NVCs and an extensive set of 360-degree projection formats with respect to their compression performance for 360-degree video. Based on our analysis, we find that projection format resampling yields significant improvements in compression performance also for NVCs. The adjusted cubemap projection (ACP) and equatorial cylindrical projection (ECP) show to perform best and achieve rate savings of more than 55% compared to ERP based on WS-PSNR for the most recent NVC. Remarkably, the observed rate savings are higher than for H.266/VVC, emphasizing the importance of projection format resampling for NVCs.

**Index Terms**—learned video compression, 360-degree, video coding, projection format resampling

## I. INTRODUCTION

The task of video compression is a crucial element of today’s multimedia communications landscape. Among the most prominent video compression standards are hybrid video codecs like the popular H.264/AVC [1], its successor H.265/HEVC [2], and the state-of-the-art H.266/VVC [3].

With the growing popularity of augmented and virtual reality systems (AR/VR), the importance of efficient video compression especially of 360-degree video content further increases. In order to use existing, highly efficient video compression standards, 360-degree videos need to be mapped to the 2D image plane prior to encoding leading to inevitable distortions [4]. Special efforts in improving compression performance for 360-degree video include the design of improved projection formats [5] and the development of 360-degree specific coding tools [6]–[10].

In recent years, neural video compression networks (NVCs) have experienced significant advances [11]–[16] and already

This work was supported by the Deutsche Forschungsgemeinschaft (DFG, German Research Foundation) under project number 418866191.

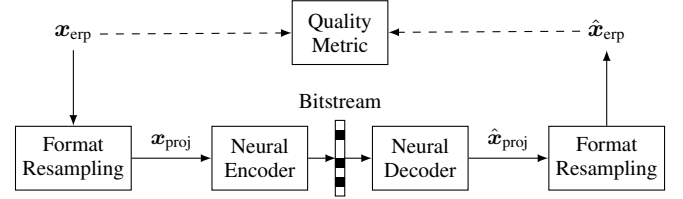


Fig. 1. Investigated coding framework with the original video  $x_{erp}$  in equirectangular projection and the resampled video  $x_{proj}$  in coding projection.  $\hat{x}_{proj}$  and  $\hat{x}_{erp}$  are the corresponding decoded videos.

perform close to state-of-the-art video compression standards like H.266/VVC that have evolved over decades. These fast-paced improvements suggest that neural network based video coding technologies will become increasingly important in the future. However, evaluations of NVC compression performance have so far mainly addressed perspective content. It is thus unclear, how NVCs behave for 360-degree video in different projection formats and whether specific extensions for 360-degree video are required, as is the case for hybrid video codecs.

This paper aims to provide clarity on these points by analysing the compression performance of NVCs for 360-degree video. Similar to the investigations for hybrid video codecs, an extensive set of 360-degree projection formats is tested and compared with respect to their compression performance. Fig. 1 shows an overview of our NVC testing framework that follows the process proposed by the Joint Video Experts Team (JVET) in the common test conditions for 360-degree video [17]. In addition to showing that projection format resampling becomes even more important for NVCs than it has been for H.266/VVC, we show that its importance is likely to increase even further in future NVCs, based on trends derived from testing multiple generations of NVCs.

## II. INVESTIGATED NETWORKS AND PROJECTION FORMATS

### A. Deep Contextual Video Compression Networks

**DCVC:** The deep contextual video compression network [13] employs a conditional coding framework. Hybrid video codecs employ a residual coding framework, where a prediction is generated based on additional side information,

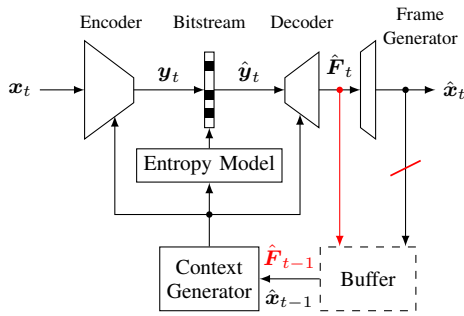


Fig. 2. Schematic of DCVC and its extensions. Elements in red show the updated feature buffer introduced with DCVC-TCM.  $x_t$  describes the input frame,  $y_t$  the latent space,  $\hat{y}_t$  the decoded latent space,  $\hat{F}_t$  the last feature of the decoder and  $\hat{x}_t$  the decoded frame at time step  $t$ .

subtracted from the current input signal, and only the residual signal is coded. Conditional coding differs from residual coding by directly providing the given side information to the individual network components allowing them to flexibly learn the relevant features for efficient coding. Fig. 2 shows a simplified schematic of the basic DCVC framework. The buffered frame from the last time step  $\hat{x}_{t-1}$  is further processed in a context generation network and the learned context is then provided to the individual network components. Motion estimation and motion compensation are omitted for readability. Note, however, that the context generator uses motion information to warp the learned features internally. The entropy model includes a hyperprior model, employs an autoregressive component for spatial correlation, and is conditioned on the learned context for temporal correlation.

**DCVC-TCM:** As an extension to DCVC, DCVC-TCM [14] includes a temporal context mining module and discards the autoregressive component in the entropy model for faster decoding. As shown in red in Fig. 2, instead of using the last decoded frame  $\hat{x}_{t-1}$  for context generation, the temporal context mining module generates context from the last feature  $\hat{F}_{t-1}$  before the last convolutional layer of the frame generator. It performs a multi-scale procedure to generate context at multiple scales. Motion information is used at the multiple scales to warp learned features accordingly. The resulting multi-scale temporal contexts are inserted into the encoder, decoder and entropy model networks at the respective scales at different stages of the networks.

**DCVC-HEM:** By improving the entropy model and allowing a multi-granularity quantization, DCVC-HEM [15] further improves upon DCVC-TCM. The hybrid spatial-temporal entropy model splits the channels of the latent space and then performs a parallel two-step checkerboard coding. In the first step, only the even/odd positions of both channel splits are coded based on the available multi-scale temporal contexts, a hyperprior and the last decoded latent space  $\hat{y}_{t-1}$ . In the second step, the entropy model is additionally conditioned on the spatial information from the first coding step allowing spatial correlation and codes the odd/even positions

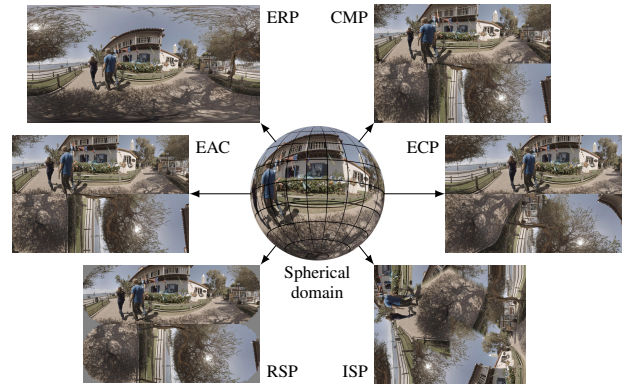


Fig. 3. Overview of a subset of projection formats including the equirectangular (ERP), cubemap (CMP), equiangular cubemap (EAC), equatorial cylindrical (ECP), rotated sphere (RSP), and icosahedron (ISP) projection.

of both channels. The multi-granularity quantization allows to adjust rate in a single network without having to train different models for different rate points. It contains three quantization steps including global quantization based on user input, a fixed learned channel-wise quantization, and a content-adaptive learned spatial-channel-wise quantization.

**DCVC-DC:** Most notable advancements of DCVC-DC [16] over DCVC-HEM include the improvement of the context generation enabling long-term context and a quadtree-based entropy model. The modified architecture of the context generation network employs the idea of offset diversity for internal motion compensation, where features are warped at multiple motion vector offsets. Features warped at the same offset are called a group. A so-called cross-group fusion network then learns context by combining features from multiple groups in a parallelization friendly manner. The cross-group fusion network also includes a skip connection throughout of the last feature  $\hat{F}_{t-1}$ , which allows to learn long-term context over multiple frames. The quadtree entropy coding improves upon the two-step coding method from DCVC-HEM by splitting channels in four parts, and coding spatial positions in a quadtree. The resulting four-step procedure increases spatial and channel-wise correlation leading to improved coding efficiency.

### B. 360-Degree Projection Formats

**Equirectangular-based (ERP, AEP):** The mapping of the classical *equirectangular projection* (ERP) is identical to the mapping of a classical world map, where the longitudes and latitudes are mapped to the horizontal and vertical image axes, respectively (cf. Fig. 3). Due to its simplicity, ERP is one of the most common projection formats. Unlike many projection formats, it entails no discontinuous face boundaries as it consists of a single homogeneous face. However, this comes at the cost of strong nonlinear distortions especially in the vicinity of the poles. The *adjusted equalarea projection* (AEP) [18] is a modification of ERP that alters the sampling rate along the latitudinal direction to better preserve the area of objects in the spherical domain representation.

**Cubemap-based (CMP, EAC, HEC, ACP, GCP):** The *cubemap projection (CMP)* is derived by projecting the 360-degree image onto the faces of a cube surrounding the image sphere in the spherical domain. To map a pixel coordinate on the image sphere to a position on the cube, a light ray from the origin to the regarded pixel coordinate is formulated. The intersection of this light ray with the surrounding cube defines the mapped pixel position. The six resulting cube faces are arranged onto a 2D plane such that face discontinuities are minimized as much as possible. As the pixels on the cube faces are arranged in a homogeneous grid, the angular distance between pixel positions on the image sphere decreases with increasing distance to the center of each cube face. The *equiangular cubemap projection (EAC)* [19] ensures consistent angular spacing by warping the cube faces accordingly. The *hybrid equiangular cubemap projection (HEC)* [20] follows similar goals, but adapts the vertical warping function for cube faces along the equator. Similarly, the *adjusted cubemap projection (ACP)* [21] and the *generalized cubemap projection (GCP)* [22] use modified face warping functions.

**Others (ECP, RSP, ISP):** The *equatorial cylindrical projection (ECP)* [23] yields a single homogeneous face by wrapping a cylinder around the image sphere in longitudinal direction. Pixel positions up to a specified latitudinal distance from the equator are mapped to this face. The remaining pixel positions are mapped to the top and bottom caps of the cylinder and warped to fill a rectangular area. The faces are then split and arranged onto a 2D plane similar to cubemap-based projections. The *rotated sphere projection (RSP)* [24] wraps the image sphere by two segments matching those of a tennis ball, the *icosahedron projection (ISP)* [25] wraps the image sphere by an icosahedron with 20 faces. The segments or faces are then arranged space-savingly on the 2D image plane.

### III. ANALYTICAL METHODS

#### A. Test Sequences

For our evaluations, we use the JVET 360-degree test sequences [17]. The dataset consists of 10 uncompressed sequences in ERP format in yuv color space with 4:2:0 chroma subsampling. Resolutions range from 6K to 8K with frame rates of 30 to 60 fps and bit depths of 8 and 10 bit. 32 frames of each sequence are tested.

#### B. 360-Degree Projection Format Resampling

As all test sequences are in ERP format, a projection format resampling is necessary to evaluate the compression performance of the individual projection formats. We follow the common test conditions for 360-degree video (360-CTC) [17] and use 360Lib-13.1 [26] for all described operations as used in standardization. As visualized in Fig. 1, the resampling is performed before encoding and reversed after decoding. This allows to perform quality metric evaluation in the ERP domain independent of the respective projection format used for coding. The resampling procedure combines downsampling to roughly 2K, projection format resampling, and conversion

to 4:4:4 chroma subsampling. The downsampled resolution is selected as  $2048 \times 1024$  for ERP, AEP,  $1800 \times 1200$  for CMP, EAC, HEC, ACP, ECP, RSP,  $1816 \times 1232$  for GCP, and  $1306 \times 1672$  for ISP. As noted in the 360-CTC, downsampling ensures that ERP has no unfair advantage against other projection formats. After decoding, the decoded sequence is resampled back to the original ERP format, resolution and 4:2:0 chroma subsampling.

#### C. Video Codec Implementations

For the investigated NVCs described in Section II-A, the open source implementations and pretrained network weights [27] published by the original authors are employed. As we focus on analyzing the compression capabilities using general purpose network weights, a finetuning to 360-degree video is explicitly not performed. The available network weights have been trained on the Vimeo-90K dataset [28]. For DCVC and DCVC-TCM, different rate points (rate-distortion-tradeoffs) are achieved through different sets of pretrained network weights. For DCVC-HEM and DCVC-DC, different rate points are achieved with the same set of pretrained network weights by varying a quality parameter. We homogenize the two concepts by defining a quality index  $q \in \{0, 1, 2, 3\}$  ranging from low- to high-bitrate scenarios. Depending on the selected quality index  $q$  and the regarded NVC, the required set of pretrained network weights are loaded or the according quality parameter is set. All employed network weights were pretrained on a mean squared error (MSE) distortion loss. The group of pictures (GOP) is set as 32. All networks code in RGB color space. Color space conversion from YUV 4:4:4 color space to RGB color space and vice versa is performed before and after decoding according to BT.709 [29].

For H.266/VVC, VTM-22.2 [30] is employed in low-delay (LD) configuration similar to [16]. Instead of different quality indices  $q$ , different rate points are selected through the quantization parameter  $QP \in \{22, 27, 32, 37\}$  ranging from high- to low-bitrate scenarios. All remaining elements of the testing framework remain unaltered.

#### D. Performance Evaluation

To evaluate the different combinations of 360-degree projection formats and NVCs, the achieved rate distortion performance needs to be assessed. The rate is obtained as the average bits per pixel of the compressed bitstream. As distortion metrics, PSNR and WS-PSNR [31] are used. WS-PSNR is an extension of PSNR for 360-degree video that weights the error at each pixel position by the area it covers in the spherical domain. Both metrics are calculated between the original video  $x_{erp}$  and the decoded video  $\hat{x}_{erp}$  in ERP format and YUV 4:2:0 color space as shown in Fig. 1. YUV-PSNR and YUV-WS-PSNR are calculated by weighting the PSNR of the three YUV components as  $(w_y, w_u, w_v) = (6, 1, 1)/8$  matching the evaluation procedure in standardization [32]. The achieved rate distortion performance is evaluated using the Bjøntegaard Delta (BD) model [33].

TABLE I

PER-CODEC BD-RATE IN % FOR THE DIFFERENT PROJECTION FORMATS WITH RESPECT TO ERP BASED ON YUV-PSNR AND YUV-WS-PSNR. ENTRIES MARKED BY \* WERE CALCULATED WITH AN INTERSECTION OVER UNION OF BOTH RATE DISTORTION CURVES OF LESS THAN 33%. LOWER IS BETTER.

		ERP	AEP	CMP	EAC	HEC	ACP	GCP	ECP	RSP	ISP
YUV-PSNR	VTM-22.2	0.00	-1.70	-2.33	-25.93	-24.85	-27.78	-26.14	-23.17	-22.24	82.08
	DCVC	0.00	0.48	4.12	-14.79	-15.44	-15.30	-11.54	-13.61	-13.13	43.72
	DCVC-TCM	0.00	0.69	0.84	-28.24	-27.03	-29.05	-26.46	-25.31	-23.59	75.64
	DCVC-HEM	0.00	0.42	-4.79	-37.37	-36.17	-38.12	-36.19	-35.53	-31.44	95.36
	DCVC-DC	0.00	0.41	-10.32	-42.62*	-41.65*	-43.54*	-42.49*	-40.35	-36.05	106.51
YUV-WS-PSNR	VTM-22.2	0.00	-20.66	-22.49	-37.84	-37.21	-39.07	-38.16	-37.58	-34.44	-18.31
	DCVC	0.00	-14.90	-13.99	-26.41	-27.36	-26.59	-23.93	-27.62	-24.83	-10.01
	DCVC-TCM	0.00	-21.87	-23.43	-42.74	-42.23	-42.90	-41.45	-42.94	-38.63	-21.02
	DCVC-HEM	0.00	-28.12	-31.70	-52.48*	-51.85*	-52.60*	-51.83*	-53.36*	-46.97*	-30.35
	DCVC-DC	0.00	-29.66	-35.41	-56.20*	-55.71*	-56.42*	-56.39*	-56.67*	-50.09*	-33.97

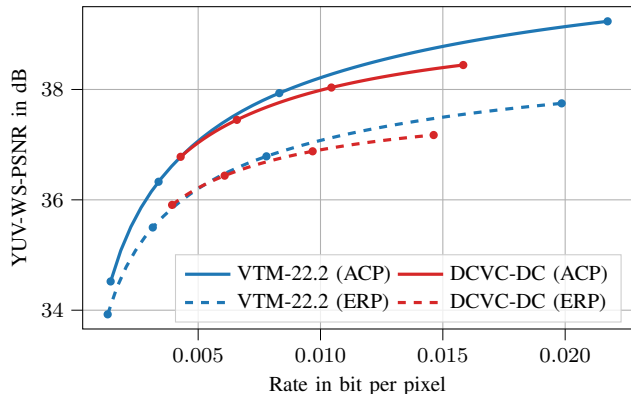


Fig. 4. Rate distortion performance of VTM-22.2 (blue) and DCVC-DC (red) for ERP (dashed) and ACP (solid) formats.

#### IV. EXPERIMENTAL RESULTS

For classical hybrid video codecs, significantly improved compression performance can be achieved by resampling 360-degree videos in ERP format to different projection formats for coding. For NVCs, it has not yet been investigated if projection format resampling yields rate savings as well, how large the potential rate savings are, and how the different projection functions behave compared to the behavior for hybrid video codecs. In the following, we aim to answer these questions.

Table I shows the BD-Rate of VTM-22.2 and the described NVCs for the different projection formats. The anchor is selected as ERP for each codec individually, i.e., the BD-Rates are calculated independently for each row. The BD-Rates are shown for both YUV-PSNR and YUV-WS-PSNR as quality metrics, which we abbreviate as PSNR and WS-PSNR in the following. Entries marked by \* were calculated with an intersection over union (IoU) of less than 33% of both rate distortion curves along the distortion (quality) metric axis and should thus be treated with caution.

Fig. 4 provides an example of this behavior showing the rate distortion curves for VTM-22.2 and DCVC-DC for the ERP and ACP formats. While the curves for VTM-22.2 have sufficient overlap, the curves for DCVC-DC have an IoU of less than 33% along the distortion axis. The corresponding BD-Rate value is thus marked by \*. Clearly, the overlap of the

curves for DCVC-DC is much larger along the rate axis. For this reason, all statements based on BD-Rate values marked by \* have been cross-checked using BD-PSNR and BD-WS-PSNR to confirm their validity.

For both BD-Rates based on PSNR and WS-PSNR shown in Table I, projection format resampling shows significant gains in compression performance compared to coding in ERP format across all codecs. For our initial investigations, we focus on DCVC-DC as the most recent NVC. With average rate savings of more than 55% based on WS-PSNR and more than 40% based on PSNR, the EAC, HEC, ACP, GCP and ECP projection formats perform best. Overall, ACP and ECP yield the highest rate savings based on WS-PSNR, though ACP clearly outperforms ECP based on PSNR. RSP follows closely with rate savings of roughly 50% based on WS-PSNR and 36% based on PSNR. The AEP, CMP and ISP formats cannot compete. This ranking of projection formats is consistent across all investigated NVC generations.

The EAC, HEC, ACP, GCP and ECP formats have in common that their individual faces exhibit distortions close to those occurring in conventional perspective video, while also being modified to reduce face boundary discontinuities. If these discontinuities are not adequately taken care of, the compression performance of both VTM-22.2 and the different NVCs suffers noticeably, as visible for the CMP and ISP formats, which show only piecewise perspective characteristics.

It is remarkable that the observed rate savings by applying a reprojection are higher for most NVCs than for VTM-22.2. For example, while ACP achieves rate savings of more than 56% based on WS-PSNR for DCVC-DC, rate savings of less than 40% are achieved for VTM-22.2. This shows the increased importance of projection format resampling in the context of NVCs.

Investigating the different generations of NVCs, we find that the gap in compression performance between ERP and other formats is steadily increasing, caused by the ongoing specialization of NVCs onto perspective content. If research on NVCs continues to focus on perspective video, the importance of projection format resampling is thus likely to increase even further in future NVC generations. However, similar to H.266/VVC that contains specific extensions for 360-degree video, the investigation of specific extensions in NVCs might

be a promising approach to further increase compression performance, as well. Possible approaches could be to finetune network weights for different 360-degree projections, or to investigate 360-degree specific modifications of the internal network architecture.

## V. CONCLUSION

In this paper, the compression performance of neural video compression networks (NVCs) is analyzed for their application to 360-degree video coding. For the evaluation, different generations of NVCs are investigated with respect to their performance on different 360-degree projection formats. In the context of NVCs, our results show that projection formats like ACP and ECP whose individual faces more closely replicate the characteristics of perspective video, while also considering the reduction of face boundary discontinuities, perform best. Rate savings of more than 55% compared to coding in ERP format are observed, showing even higher gains than for H.266/VVC. Throughout the different NVC generations, the increasing compression performance for perspective content translates into steadily increasing gains of projection formats like ACP and ECP compared to ERP. Based on the presented results, many promising directions for future research open up. Possibilities include the optimization of projection format parameters during network training to derive improved projection formats with even higher rate savings, investigating the potential gains if a network is finetuned on 360-degree content in different projection formats, or specifically adapting the network architectures to better handle 360-degree video.

## REFERENCES

- [1] T. Wiegand, G.J. Sullivan, G. Bjontegaard, and A. Luthra, "Overview of the H.264/AVC Video Coding Standard," *IEEE Trans. Circuits Syst. Video Technol.*, vol. 13, no. 7, pp. 560–576, July 2003.
- [2] Gary J. Sullivan, Jens-Rainer Ohm, Woo-Jin Han, and Thomas Wiegand, "Overview of the High Efficiency Video Coding (HEVC) Standard," *IEEE Trans. Circuits Syst. Video Technol.*, vol. 22, no. 12, pp. 1649–1668, Dec. 2012.
- [3] Benjamin Bross, Ye-Kui Wang, Yan Ye, Shan Liu, Jianle Chen, Gary J. Sullivan, and Jens-Rainer Ohm, "Overview of the Versatile Video Coding (VVC) Standard and its Applications," *IEEE Trans. Circuits Syst. Video Technol.*, vol. 31, no. 10, pp. 3736–3764, Oct. 2021.
- [4] I. I. Pearson, *Map Projections: Theory and Applications*, CRC Press, Boca Raton, Fla, 2nd edition edition, Mar. 1990.
- [5] Yan Ye and Jill Boyce, "Algorithm Descriptions of Projection Format Conversion and Video Quality Metrics in 360Lib Version 12, JVET-T2004-v2," in *Proc. 20th Meet. Jt. Video Experts Team*, Oct. 2020, pp. 1–65.
- [6] Johannes Sauer, Jens Schneider, and Mathias Wien, "Improved Motion Compensation for 360° Video Projected to Polytopes," in *Proc. IEEE Int. Conf. Multimed. Expo*, July 2017, pp. 61–66.
- [7] Johannes Sauer, Mathias Wien, Jens Schneider, and Max Blaser, "Geometry-Corrected Deblocking Filter for 360° Video Coding using Cube Representation," in *Proc. Pict. Coding Symp.*, June 2018, pp. 66–70.
- [8] Yimin Zhou, Ling Tian, Ce Zhu, Xin Jin, and Yu Sun, "Video Coding Optimization for Virtual Reality 360-Degree Source," *IEEE J. Sel. Top. Signal Process.*, vol. 14, no. 1, pp. 118–129, Jan. 2020.
- [9] Bharath Vishwanath, Tejaswi Nanjundaswamy, and Kenneth Rose, "A Geodesic Translation Model for Spherical Video Compression," *IEEE Trans. Image Process.*, vol. 31, pp. 2136–2147, Feb. 2022.
- [10] Andy Regensky, Christian Herglotz, and André Kaup, "Multi-Model Motion Prediction for 360-Degree Video Compression," *IEEE Access*, vol. 11, pp. 117004–117017, Oct. 2023.
- [11] Guo Lu, Wanli Ouyang, Dong Xu, Xiaoyun Zhang, Chunlei Cai, and Zhiyong Gao, "DVC: An End-To-End Deep Video Compression Framework," in *Proc. IEEE/CVF Conf. Comput. Vis. Pattern Recognit.*, June 2019, pp. 10998–11007.
- [12] Eirikur Agustsson, David Minnen, Nick Johnston, Johannes Balle, Sung Jin Hwang, and George Toderici, "Scale-Space Flow for End-to-End Optimized Video Compression," in *Proc. IEEE/CVF Conf. Comput. Vis. Pattern Recognit.*, June 2020, pp. 8500–8509.
- [13] Jiahao Li, Bin Li, and Yan Lu, "Deep Contextual Video Compression," in *Proc. Adv. Neural Inf. Process. Syst.*, 2021, vol. 34, pp. 18114–18125.
- [14] Xihua Sheng, Jiahao Li, Bin Li, Li Li, Dong Liu, and Yan Lu, "Temporal Context Mining for Learned Video Compression," *IEEE Trans. Multimed.*, vol. 25, pp. 7311–7322, 2023.
- [15] Jiahao Li, Bin Li, and Yan Lu, "Hybrid Spatial-Temporal Entropy Modelling for Neural Video Compression," in *Proc. 30th ACM Int. Conf. Multimed.*, New York, NY, USA, Oct. 2022, MM '22, pp. 1503–1511.
- [16] Jiahao Li, Bin Li, and Yan Lu, "Neural Video Compression With Diverse Contexts," in *Proc. IEEE/CVF Conf. Comput. Vis. Pattern Recognit.*, 2023, pp. 22616–22626.
- [17] Yuwen He, Jill Boyce, Kiho Choi, and Jian-Liang Lin, "JVET Common Test Conditions and Evaluation Procedures for 360° Video, JVET-U2012," in *Proc. 21st Meet. Jt. Video Explor. Team*, Jan. 2021, pp. 1–8.
- [18] Minhua Zhou, "AHG8: A Study On Quality Impact of Line Re-Sampling Rate in EAP, JVET-G0051," in *Proc. 7th Meet. Jt. Video Explor. Team*, July 2017, pp. 1–5.
- [19] Minhua Zhou, "AHG8: A Study on Equi-Angular Cubemap Projection (EAC), JVET-G0056," in *Proc. 7th Meet. Jt. Video Explor. Team*, July 2017, pp. 1–14.
- [20] Ya-Hsuan Lee, Jian-Liang Lin, Shen-Kai Chang, and Chi-Cheng Ju, "CE13: Modified Cubemap Projection in JVET-J0019 (Test 5), JVET-K0131," in *Proc. 11th Meet. Jt. Video Explor. Team*, July 2018, pp. 1–6.
- [21] Muhammed Coban, Geert Van der Auwera, and Marta Karczewicz, "AHG8: Adjusted Cubemap Projection for 360-Degree Video, JVET-F0025," in *Proc. 6th Meet. Jt. Video Explor. Team*, Apr. 2017, pp. 1–6.
- [22] Ya-Hsuan Lee, Jian-Liang Lin, Ying-Jui Chen, Chi-Cheng Ju, Jill Boyce, and Max Dmitrichenko, "AHG6/AHG17: Generalized Cubemap Projection Syntax for 360-Degree Videos," in *Proc. 16th Meet. Jt. Video Experts Team*, Nov. 2019, pp. 1–12.
- [23] Geert Van der Auwera, Muhammed Coban, and Marta Karczewicz, "AHG8: ECP with Padding for 360-Degree Video, JVET-G0074," in *Proc. 7th Meet. Jt. Video Explor. Team*, July 2017, pp. 1–14.
- [24] Adeel Abbas and David Newman, "AHG8: Rotated Sphere Projection for 360 Video, JVET-F0036," in *Proc. 6th Meet. Jt. Video Explor. Team*, Apr. 2017, pp. 1–7.
- [25] Vladislav Zakharchenko, Elena Alshina, Kwang Pyo Choi, Minseok Choi, Amith Dsouza, and Anubhav Singh, "AHG8: Icosahedral Projection for 360-Degree Video Content, JVET-D0028," in *Proc. 4th Meet. Jt. Video Explor. Team*, Oct. 2016, pp. 1–5.
- [26] JVET, "360Lib Software 360Lib-13.1," <https://vcgit.hhi.fraunhofer.de/jvet/360lib/-/tags/360Lib-13.1>, Oct. 2021.
- [27] Microsoft, "DCVC Github Repository," <https://github.com/microsoft/DCVC>, Nov. 2023.
- [28] Tianfan Xue, Baian Chen, Jiajun Wu, Donglai Wei, and William T. Freeman, "Video Enhancement with Task-Oriented Flow," *Int. J. Comput. Vis.*, vol. 127, no. 8, pp. 1106–1125, Aug. 2019.
- [29] ITU-R, "Rec. ITU-R BT.709-6: Parameter Values for the HDTV Standards for Production and International Programme Exchange," June 2015.
- [30] JVET, "VVC Reference Software VTM-22.2," [https://vcgit.hhi.fraunhofer.de/jvet/VVCSoftware\\_VTM/-/releases/VTM-22.2](https://vcgit.hhi.fraunhofer.de/jvet/VVCSoftware_VTM/-/releases/VTM-22.2), Oct. 2023.
- [31] Yule Sun, Ang Lu, and Lu Yu, "Weighted-to-Spherically-Uniform Quality Evaluation for Omnidirectional Video," *IEEE Signal Process. Lett.*, vol. 24, no. 9, pp. 1408–1412, Sept. 2017.
- [32] ITU-T, "Working Practices Using Objective Metrics for Evaluation of Video Coding Efficiency Experiments," July 2020.
- [33] Gisle Bjontegaard, "Calculation of Average PSNR Differences between RD-curves, VCEG-M33," in *Proc. 13th Meet. Video Coding Experts Group*, Mar. 2001, pp. 1–5.